COMPARISON BETWEEN AN ELECTROCHEMICAL REACTOR WITH AND WITHOUT MEMBRANE FOR THE NOR OXIDATION USING NOVEL CERAMIC ELECTRODES

J. Carrillo-Abad[1], J. Mora-Gómez[1], M. García-Gabaldón[1], S. Mestre[2], V. Pérez-Herranz[1].

1) IEC Group, Universitat Politècnica de València, Camí de Vera s/n, 46022, València, Spain

2) Instituto de Tecnología Cerámica, Campus Universitario Riu Sec, Av.Vicent Sos Baynat s/n, 12006, Castelló, Spain

Corresponding author: jorcarab@upvnet.upv.es

Abstract

The electrochemical oxidation of the antibiotic Norfloxacin (NOR) in chloride media on different anodic materials was studied at two different electrochemical reactors. The results were compared with those obtained in sulphate media. The anodes under study were a commercial boron-doped diamond (BBD) and two different ceramic electrodes based on tin oxide doped with antimony oxide in the presence (CuO) and absence (BCE) of copper oxide as sintering aid. The reactors employed were a one-compartment reactor (OCR) and a two-compartment one with a membrane separating both electrodes (EMR). The use of the membrane clearly enhanced both NOR degradation and TOC mineralization for all the anodic materials studied since some parallel reactions were avoided. Additionally, two different pathways for NOR oxidation were observed as a function of the reactor employed. The EMR also favoured the ionic by-products generation and the electrolyte dechlorination. NO_3^- increased with the oxidation power of the anode employed and it was also enhanced by the EMR use. Chloride media favours ceramic electrodes performance independently of the reactor employed as they did not generate an excess of oxidants as BDD did. The BCE electrode is an interesting alternative to BDD since although its oxidative power was lower, it presented similar current efficiency with lower energy consumption.

Keywords: Norfloxacin (NOR), boron-doped diamond (BDD) anode, ceramic anodes, electro-oxidation, electrochemical membrane reactor.

1- Introduction

Norfloxacin (NOR) is a fluoroquinoline (FQ) carboxylic acid extensively employed in the treatment of infectious diseases, as cattle growth promotor and in aquaculture (da Silva et al., 2018; Huang et al., 2008; Mora-Gómez et al., 2018). This FQ has become an emerging pollutant (EP) because of the inefficiency of its treatment at conventional wastewater treatment plants. Its presence in body waters, whose concentration has increased during these last years, appears as a risk to human health (da Silva et al., 2018; Jojoa-Sierra et al., 2017; Ma et al., 2018). Consequently, new advanced oxidation processes must be developed to treat these kinds of contaminants. Among them, the electrochemical-oxidation (ELOX) of refractory organic compounds showed a very good performance (Ghernaout et al., 2011; Guzmán-Duque et al., 2014; Urtiaga et al., 2018). Furthermore, ELOX techniques show adaptability, relative low cost implementation, environmental-friendly, efficiency, no addition of chemical compounds and easy automatization (Comninellis, 2010; Jojoa-Sierra et al., 2017; Sánchez-Montes et al., 2018; Sopaj et al., 2015). Depending on the anode material and the electrolyte composition, some different oxidants such as H_2O_2, $^{\cdot}OH$, persulfate, active chlorine species, etc. can be formed (Guzmán-Duque et al., 2014; Jojoa-Sierra et al., 2017).

Among the materials employed in ELOX, boron doped diamond (BDD) anodes appear as one of the most used materials because of their good properties, but these anodes present an expensive and complex fabrication process that make them not suitable for the treatment of high effluent volumes. Then, the development of low cost electrodes emerges as an interesting alternative. Different metal oxides, based on PbO_2 or SnO_2, have been tested thanks to their good resistance to corrosion, high oxygen overpotential and low fabrication cost (Martínez-Huitle and Panizza, 2018; Santos et al., 2011; Tong et al., 2008; Wang et al., 2016; Zhao et al., 2010). However, these kinds of electrodes may present a low mechanical resistance, due to inner stresses, and/or chemical resistance, such as substrate oxidation.

In the present work, the performance of novel ceramic electrodes based on SnO_2 doped with Sb_2O_3 (basic ceramic electrode or BCE), without and with CuO (CuO electrode) as sintering aid is evaluated in chloride media, which is an anion usually present in the effluent to be treated. These results are also compared with those obtained with a commercial BDD. Furthermore, two kind of electrochemical reactors with (EMR) and without (OCR) a membrane separating the cathodic compartment from the anodic one are also analysed. The use of an electrochemical membrane reactor has been reported useful as it avoids non-desirable cathodic reactions, such as the recombination of organic by-products, the cathodic destruction of oxidants or their recombination with H_2O_2 (Brillas et al. 2009). Finally, the behaviour of these electrodes in both reactors is also compared with previous works using sulphate media (Mora-Gomez et al., 2019; Mora-Gómez et al., 2018).

2- Experimental

The one cell reactor, OCR, is based on a Pyrex glass of 250 cm^3 whereas the EMR consisted of two pyrex glasses, each with the same volume as the OCR, and with a NAFION-117 (from Dupont®) acting as cation-exchange membrane between the compartments. The OCR was filled with a 100 ppm of NOR in a sodium chloride (from Panreac®) solution of 1.64 gL^{-1}. This solution was used as anolyte in the EMR while a solution of pure electrolyte with the same concentration was employed as catholyte. Figure 1 shows a schematic representation of both reactors employed. The solutions were prepared ultrapure HPLC water (from Sigma-Aldrich® and Fisher Chemical) and they were vigorously stirred with a magnetic bar to ensure the reactants transport. NOR solutions were made from grade reagents and when employed to made patrons and from pharmaceutical pills for the electrolysis solutions. These pills were smashed, dissolved in ultrapure water and filtered using 56 µm fibre glass filters to remove excipients.

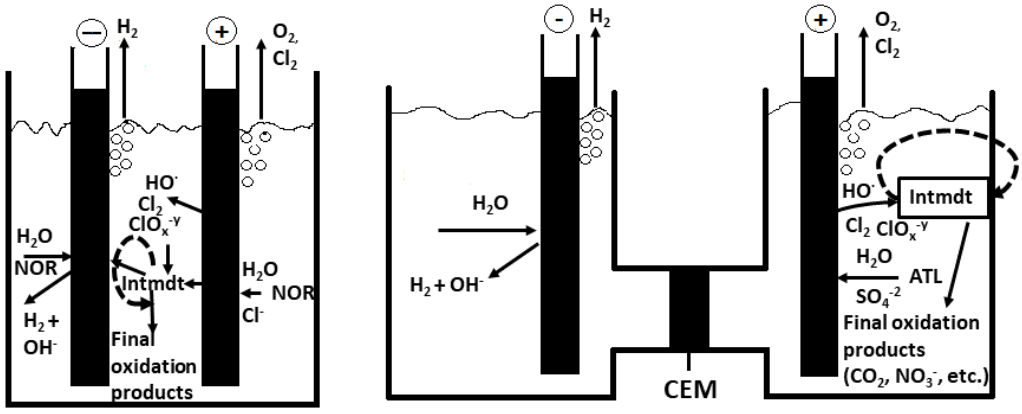

Fig. 1: Schematic representation of OCR (left) and EMR (right) including a simplified diagram of the reactions expected.

The cathode was an AISI 304 stainless steel sheet of 20 cm^2 while the reference one consisted of a standard Ag/AgCl saturated KCl electrode. Regarding the anode, three different materials were tested: a BDD with a 2500 ppm doping level (from NEOCOAT SA®, Switzerland) and two new microporous SnO_2 ceramic electrodes, both doped with Sb_2O_3 but with (CuO electrode) or without CuO (BCE electrode) as sintering agent. The contact surface for all the anodes employed was 5.28 cm^2. The synthesis of the ceramic electrodes is well explained in previous works (Mora-Gomez et al., 2019; Mora-Gómez et al., 2018). These electrodes presented a high stability and no changes not only in their surface but also in their performance as anodes were observed after an accelerated life test (Mora-Gomez et al., 2020). As shown in Table 1, SnO_2 is the main component of the ceramic matrix (purity 99.85%, Quimialmel® S.A., Spain), Sb_2O_3 as is added as a dopant (purity 99%, Alfa-Aesar®, Germany), and CuO (at Copper electrodes) as a sintering aid (purity 97%, Panreac® S.A., Spain).

Table 1: Composition (% of molar ratio) of the ceramic electrodes.

	SnO_2	**Sb_2O_3**	**CuO**
BCE	98	2	--
CuO	97.8	1	1.2

Electrooxidation experiments were carried out under galvanostatic conditions at 76 mA/cm^2 by the use of a power supply. The operation variables, such as electrode potential, cell voltage or current, were recorded during the experiment while samples were taken from the reactor each 30 min. All the experiments were performed at room temperature for 4h. NOR degradation was followed by the measure of the samples' absorbance at 275nm using a Unicam UV4-200 UV/vis spectrometer. Additionally, NOR mineralization was determined by measuring both total

organic carbon (TOC) and inorganic ions (NH_4^+, NO_3^- F^- and carboxylic acids.) using a Shimadzu TNM-L ROHS TOC analyser and Metrohm Ionic Chromatograph 883 Basic IC Plus, respectively. The products of the electrolyte oxidation (ClO_2^-, ClO_3^-, ClO_4^-) were also detected. On the other hand, the intermediates generated during the electrochemical degradation of NOR were analysed by an UHPLC coupled with a quadrupole time-of-flight mass spectrometer (UHPLC-QTOF-MS/MS). Both UHPLC and QTOF facilities were from Agilent, 1290 Infinity II liquid chromatography system and 6530 Q-TOF LC/MS, respectively. Statistical data and compound identification were carried out by Agilent Mass Hunter software.

In order to compare the performance of all the anodic materials together with the type of reactor employed some electrochemical parameters were calculated such as the extent of electrochemical combustion (ϕ_{Zn}), the mineralization current efficiency (MCE) and the specific energy consumption (E_s) (Coledam et al., 2018, 2016; da Silva et al., 2018; Guinea et al., 2010; Mora-Gomez et al., 2019).

The first one, ϕ_{NOR}, represents the NOR fraction that is completely mineralized and is obtained as follows:

$$\emptyset = \frac{\%TOC_{removal}}{\%NOR_{removal}} \quad (1)$$

This parameter varies from 0 to 1, where the 0 indicates a process without combustion while a 1 represents a complete mineralization.

Regarding MCE, it shows how much current is used in the TOC mineralization for a given time t (min) in relation to the total current applied, and is calculated as follows:

$$MCE = \frac{nFV\Delta(TOC)_t}{7.2 \cdot 10^5 mIt} \quad (2)$$

where F is the Faraday constant, V is the volume of the reactor (in L), I is the applied current (A), $\Delta(TOC)_t$ is the removed total organic carbon (mg C · L^{-1}) at a given time, m is the number of C

atoms in a NOR molecule (16), $7.2 \cdot 10^5$ is the conversion factor for the units homogenization ($60\ s \cdot min^{-1} \cdot 12000\ mg\ C\ mol^{-1}$), and n is the number of electrons transferred in the mineralization process which was assumed as 90 considering the complete mineralization of NOR into CO_2, F^- and NO_3^- present in reaction (3). This assumption was corroborated during the measurement of the ions generated during the experiments as will be seen at the results and discussion section, and was also observed by other authors (da Silva et al., 2018):

$$C_{16}H_{18}FN_3O_3 + 38\ H_2O \rightarrow 16\ CO_2 + 3\ NO_3^- + F^- + 94\ H^+ + 90\ e^- \quad (3)$$

Finally, E_s per unit of TOC ($kWh\ mg_{TOC}^{-1}$) is a useful tool that shows the energetic cost associated with the reactor operation. This parameter was calculated as:

$$E_s = \frac{\int_0^t U(t) \cdot I\ dt}{\Delta(TOC)_t \cdot V} \quad (4)$$

where U is the cell potential (V).

3- Results

3.1- Effect of the electrochemical reactor employed

Fig. 2 presents the C/C_0 decay profile for both reactors employed. The use of the membrane assures the NOR practical complete degradation independently of the anodic material employed. Comparing the results in the presence and absence of the membrane, it is inferred that its presence clearly enhances NOR oxidation, especially for the ceramic electrodes (Figs. 2 a) and c)).

Additionally, the UV-spectra evolution with time obtained for the EMR is shown for the electrodes under study at Figs. 3 a) - c) while this spectrum for NOR degradation at OCR with a BCE is presented at Fig. 3 d). This spectrum shows two main peaks for the initial sample, at 276

159 nm and 330 nm, related to ring absorption and the electronic transition of the quinolones
160 nitrogen atom from n → ∏* (HOMO-LUMO), respectively (Mora-Gomez et al., 2018;
161 Neugebauer et al., 2005). However, when the electrolysis began, Figs 3 a) – c) present very
162 similar results that greatly differ from the ones obtained with the OCR (Fig. 3 d)). This fact
163 suggests that the anode – cathode separation helps to homogenise the by-products formed
164 during the NOR degradation. Furthermore, the intermediates generated with the EMR did not
165 cause any interference in the NOR measurement, whose peak diminished with time, while for
166 the OCR a peak displacement from 276 to 290 nm was observed, which is associated with the
167 formation of a more chromophore substituent. Consequently, a different degradation pathway
168 for both reactors can be suggested (Woodward, 1942a, 1942b, 1941; Woodward and Clifford,
169 1941) Concerning the HOMO-LUMO peak, at 330 nm, it completely disappeared during the first
170 electrolysis instants, independently of both anodic material or reactor employed, which suggests
171 that this N atom is one of the firsts atoms affected during NOR oxidation. Conversely, a new
172 absorption peak appeared among 200 and 220 nm, independently of both reactor and material
173 used, which is related to the generation of short chain carboxylic acids (Coledam et al., 2016;
174 Mora-Gomez et al., 2018) as can also be seen in the ionic analysis section.

175

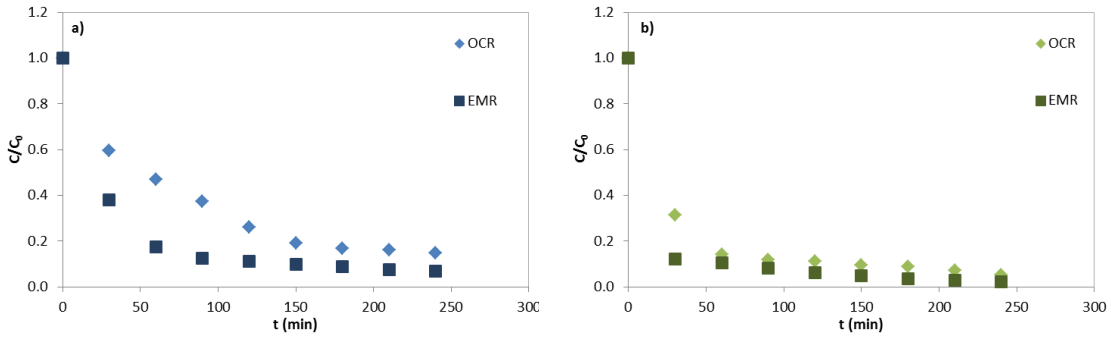

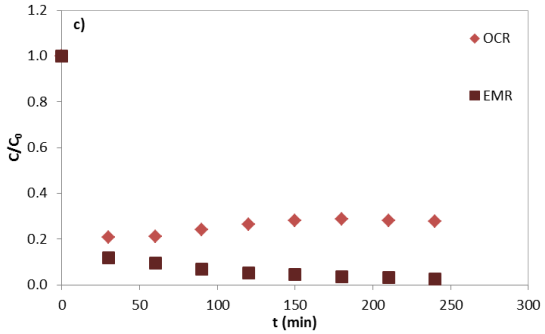

176 **Fig. 2:** C/C_0 decay profile as a function of the reactor employed (OCR and EMR) for the

177 different anode materials: CuO (a)), BDD (b)), BCE (c)).

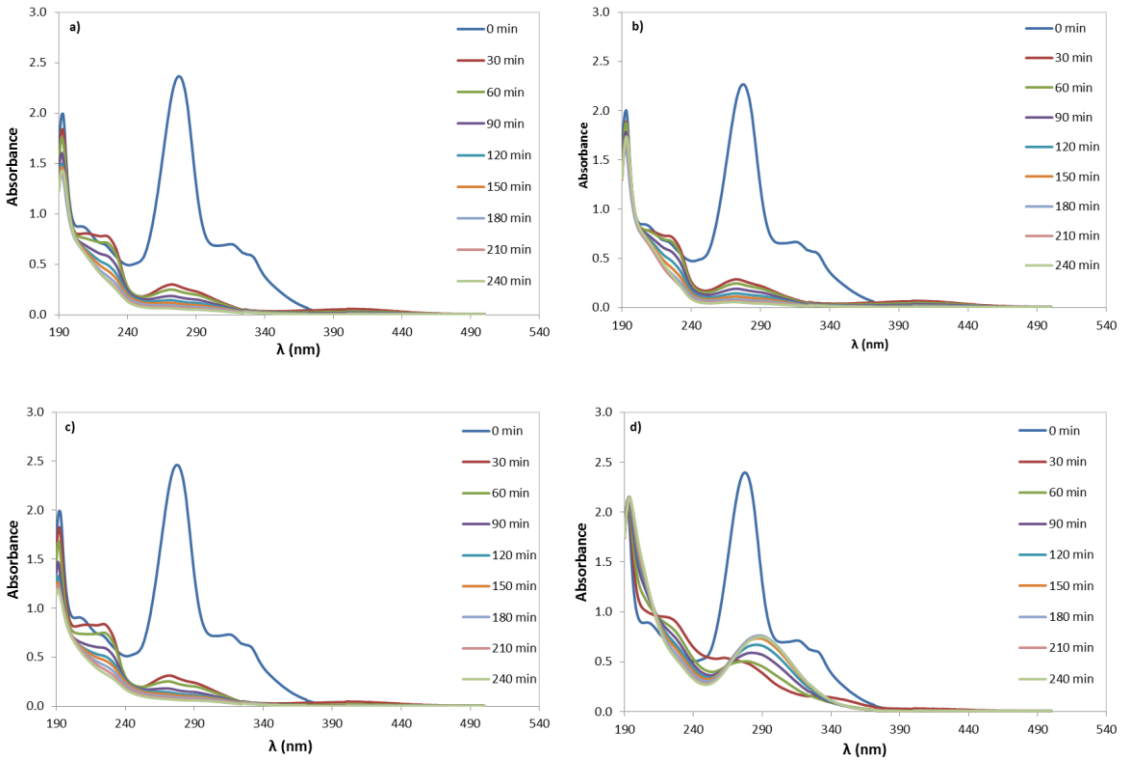

178 **Fig. 3:** UV-spectrum profile obtained as a function of the anode and reactor employed for the:

179 CuO-EMR (a)), BDD-EMR (b)), BCE-EMR (c)) and BCE-OCR (d)).

180

181 Regarding TOC evolution profile with electrolysis time, Fig. 4, it is clearly observed that the use

182 of a membrane separating cathode from anode highly improved TOC decrease for all the

183 materials tested. It may be associated with the fact that an acidic environment is formed when

184 the EMR is used, which enhances the electron transfer kinetic. Certainly, the acid dissociation

renders a precursor reaction for the electrochemical degradation pathway (Carlesi Jara et al., 2007; Mora-Gomez et al., 2019). Therefore, the membrane presence not only enhances the NOR mineralization but also changes the oxidation mechanism. This may be related to the fact that it avoids some cathodic processes, like the recombination of organic by-products (Brillas et al., 2009), the cathodic destruction of oxidants or their recombination with H_2O_2.

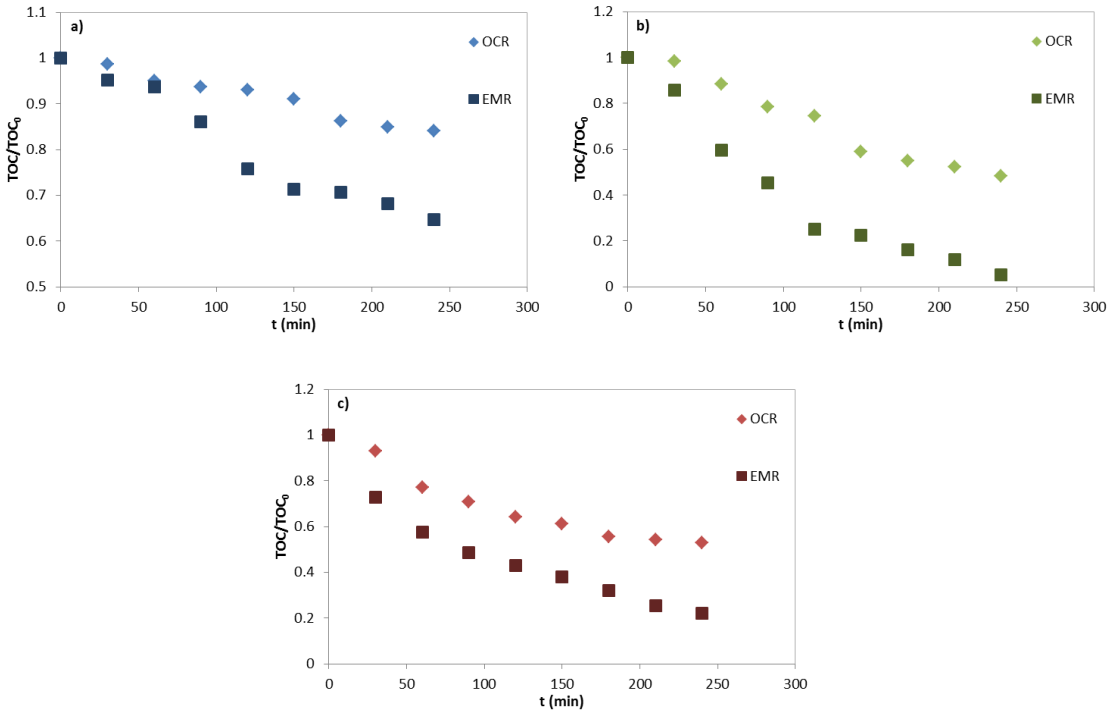

Fig. 4: TOC/TOC_0 decay profile as a function of the reactor employed (OCR and EMR) for the different anode materials: CuO (a)), BDD (b)), BCE (c)).

From both Figs. 2 and 4, it is concluded that both NOR degradation and TOC mineralization follow pseudo first order kinetics and, therefore, the values of the apparent first-order kinetic constants may be determined and are shown in Table 2. The values of k_{app} for TOC degradation are lower than those obtained for NOR degradation, as expected from Figs. 2 and 4. Comparing the values for the two kind of reactors used, it is clearly inferred that the use of a membrane

enhanced not only NOR degradation but also TOC mineralization, where the values of the apparent kinetic constant increases up to 1 order of magnitude with the use of a membrane. Regarding the oxidation power of the anodes used, the BDD appears as the most effective anode, closely followed by the BCE and, finally, the CuO is shown as the weakest anode.

Table 2: Apparent first-order kinetic constant values (min^{-1}) for NOR degradation and mineralization for each anode material and electrochemical reactor employed.

k_{app}/ Anode	CuO		BDD		BCE	
	EMR	**OCR**	**EMR**	**OCR**	**EMR**	**OCR**
NOR	*0.009*	*0.008*	*0.084*	*0.0127*	*0.072*	*
TOC	*0.0019*	*0.0007*	*0.0117*	*0.0031*	*0.0059*	*0.0031*

* This value couldn't be determined due to the interferences in NOR measurement caused by its intermediates.

3.2- Intermediates and ionic analysis

The main intermediates obtained from NOR degradation in NaCl media were determined for both reactors from the UHPLC-QTOF-MS/MS analysis. Twelve organic intermediates were identified based on the fragmentation products together with a Mass Hunter analysis. From these results, two main pathways were distinguished as a function of the reactor employed.

First of all, when the EMR was employed Fig. 5 a), the first degradation step was the defluorination of the benzene ring by a hydroxylation reaction forming the P1 compound. Afterwards, the hydroxylation of the quinolone and the benzene ring started. According to another authors, quinolone moiety is an active group that can be easily oxidized (Guo et al., 2016; Ma et al., 2018). Especially, the double bound close to quinolone group is the first one cleaved due to its proximity to a carboxylic group (I1) (Liu et al., 2012; Ma et al., 2018). Although

I1 was no detected, the P2 compound identified could come from the I1 decarboxylation. Then, another decarboxylation process generated the P3 compound that may form I2, not detected, after a decarboxylation combined with the chlorination of the quinolone N. P4 was generated after the cleavage of the ethyl group linked to the quinolone that is also substituted by a chlorine atom. Finally, the lighter product detected, P5, was formed after the loss of N from the quinolone. This P5 seems a precursor of the heaviest carboxylic acid detected from ionic chromatography, phthalate, which could be generated after the carboxylation or the chlorination of the piperazine ring.

On the other hand, the degradation pathway observed with the OCR is presented at Fig. 5 b). Any active chlorine compound attacked the secondary amine of the piperazine ring to form P'1 (C. Dodd et al., 2005), followed by a concerted fragmentation that causes the C-C bond cleavage (Jojoa-Sierra et al., 2017), generating the imine I'1, not detected. The hydrolysis of I'1 yielded to P'2 that, after the chlorination of both primary and secondary amines of the piperazine ring formed I'2, not detected, which generated P4' following the same attack scheme of P'1. Further Cl attack of the remaining N of piperazine ring together with the defluorination of the benzene ring yielded to P'5. Afterwards, the decarboxylation and the chlorine attack of the N atom of the quinolone ring generated the intermediate I'3, not detected, whose cleavage formed the lighter intermediate compound detected P'6. As commented for EMR, P'6 also seems a precursor of phthalate.

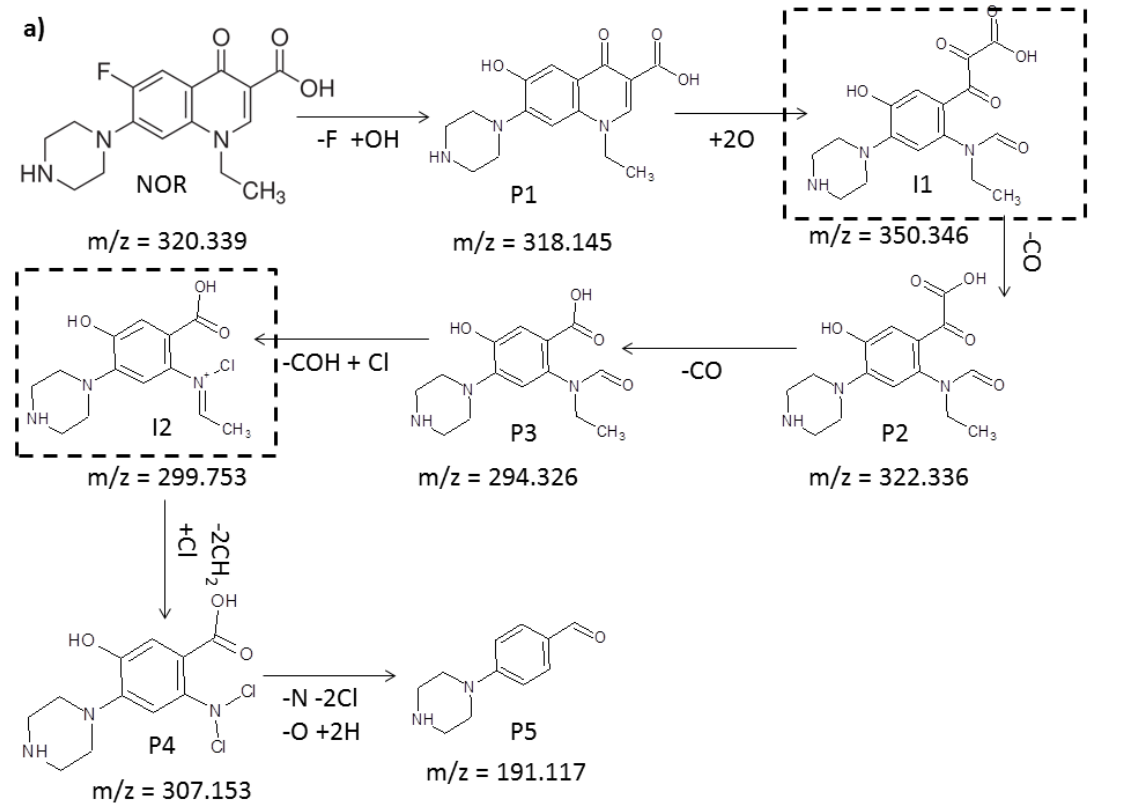

239

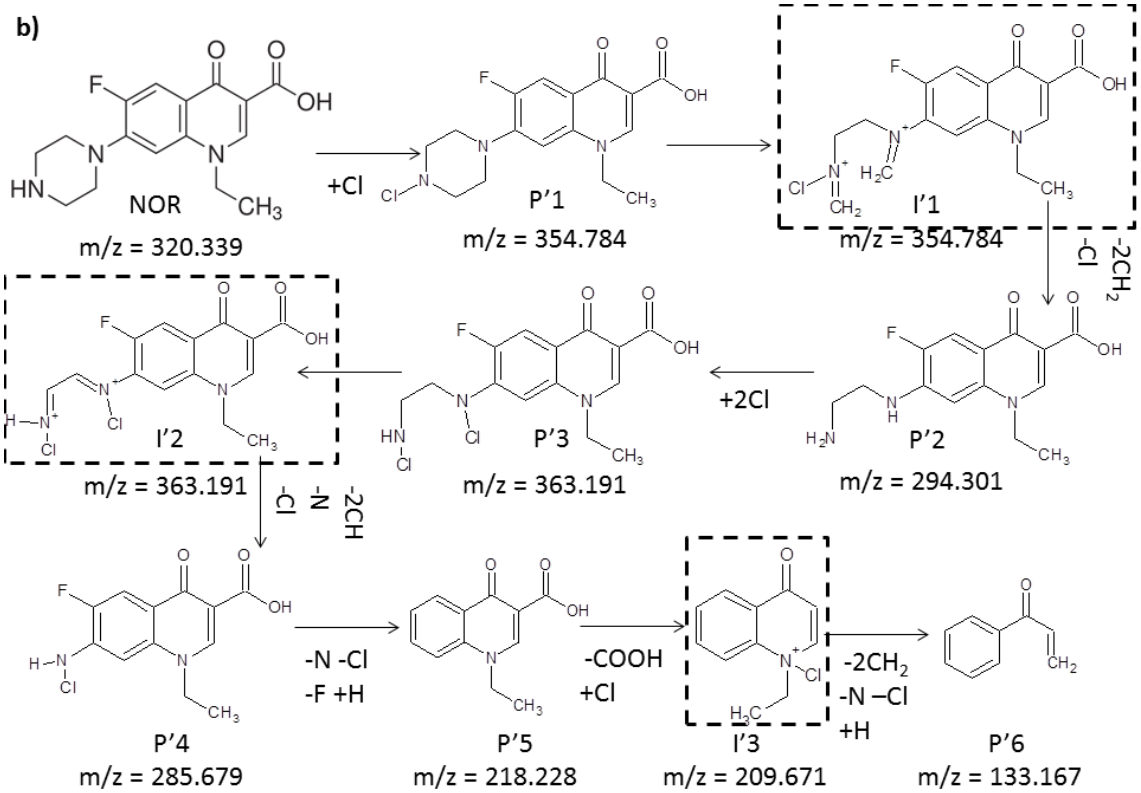

240

241 **Fig. 5:** By-products detected and degradation pathway suggested during the electrochemical

242 NOR degradation in EMR a) or OCR b).

Fig. 6 depicts the depletion percentage of the main ions generated during the NOR oxidation process, that is, denitrogenation, defluorination and the fraction of the remaining TOC associated with the carboxylic acids for all the electrodes under study with the two reactors employed. Furthermore, the dechlorination of the electrolyte was also measured. From this figure it can be concluded that the use of a membrane reactor highly enhances NOR oxidation for all the anodic materials tested.

Regarding the N-based ions generated during NOR electro-oxidation, some works detect NH_4^+ as main ion (Mora-Gomez et al., 2019; Özcan et al., 2016) while in others only NO_3^- was considered (da Silva et al., 2018). At the present study, not only no ammonium was detected but also both nitrite and nitrate were formed from the first electrolysis instants. However, depending on the anode material nitrite or nitrate was the main ion detected. BDD showed more NO_3^- ions, practically for the beginning, while for the CuO electrode NO_2^- was the main ion formed, independently of the reactor employed. Nevertheless, for the BCE depended on the reactor employed, that is, for the EMR nitrate was the main N-ion while for the OCR, was the nitrite. This may be related to the higher dechlorination obtained with the BCE-EMR, whose values were close to those obtained by the BDD-OCR since the active Cl species can oxidize N to nitrate.

Concerning the defluorination rate, the use of a membrane clearly improves its value. This may be associated with the pathways explained for each kind of reactor in Fig. 5 since at the EMR the fluoride disappeared from the very beginning while at the OCR after some degradation steps. Furthermore, the TOC remaining not only was lower in the EMR but also a higher % is caused by carboxylic acids which assured fluoride had been released to the solution.

As previously mentioned, the use of a membrane reactor favours NOR mineralization as less oxidizing species are wasted in parallel reactions and the recombination of the organic intermediates on the cathode is also avoided. Additionally, these lower TOC values are related

to the presence of carboxylic acids, which ranged from formic to phthalic, and are easily-biodegradable molecules, decreasing the toxicity of the by-products obtained.

Regarding the dechlorination levels, the use of a EMR enhances this parameter for all the materials studied as the possible reduction of chlorine species is completely avoided. Comparing the behaviour of the different materials analysed, the ceramic electrodes appears to be less effective at generating oxidative species (CuO > BCE) than the BDD one.

Finally, although the BDD anode presents the higher oxidizing power, the BCE-EMR presents results slightly higher than those obtained for the BDD-OCR, appearing the former combination as an interesting alternative.

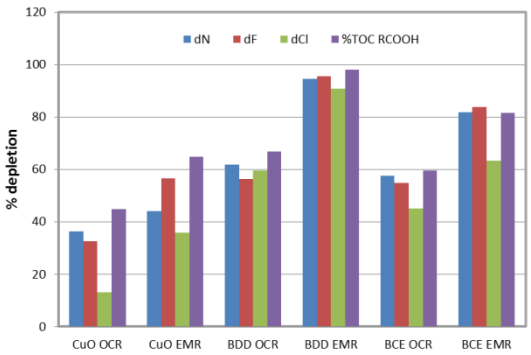

Fig. 6: % of elimination of N ions (dN), fluorine (dF), chloride (dCl) and TOC related to short chain carboxylic acids (%TOC RCOOH) after the electrolysis of NOR for each reactor and electrode material studied.

3.4- Media composition effect

Fig. 7 summarizes the effect of media composition on TOC mineralization for both reactors employed and all the anodes under study. In this point, the data regarding with sulphate media (2 g/L) for the BCE and the BDD anodes have been extracted from a previous work (Mora-Gomez et al., 2019). It is worth to note that for both ceramic electrodes, the chloride media provided

287 better results for both reactors. However, for the BDD anode, the result was completely
288 opposite with and without a membrane. This result could be related to the oxidizing power of
289 the anodes studied and the different oxidizing species formed depending on the electrolyte
290 employed. The most powerful anode was the BDD one, as discussed above. Then, the use of
291 chloride media provided more substances to be oxidized by direct and mediated oxidation. The
292 higher the amount of oxidants presents in the solution, the higher the probability of reacting
293 among themselves. Furthermore, chloride oxidation species formed some recalcitrant
294 intermediates, organic chlorinated compounds, as can be seen from Fig. 6 that could diminish
295 the oxidation power of BDD in chloride media regarding sulphate media.

296 On the other hand, the more active ceramic electrodes that cannot generate the same amount
297 of the highly oxidative sulphate and hydroxyl radicals could generate, instead of this, a higher
298 amount of chloride oxidative species which allows a higher degradation and mineralization rates
299 as chlorine active species have been demonstrated as able to degrade NOR (Jojoa-Sierra et al.,
300 2017). This different behaviour was also observed between BDD and other active electrodes,
301 such as DSA or Pt anode, where chloride media enhanced mineralization for the active electrode
302 while it slightly diminished TOC depletion for the BDD anodes (Madsen et al., 2015;
303 Murugananthan et al., 2011; Wu et al., 2009).

304

305

306

307

308

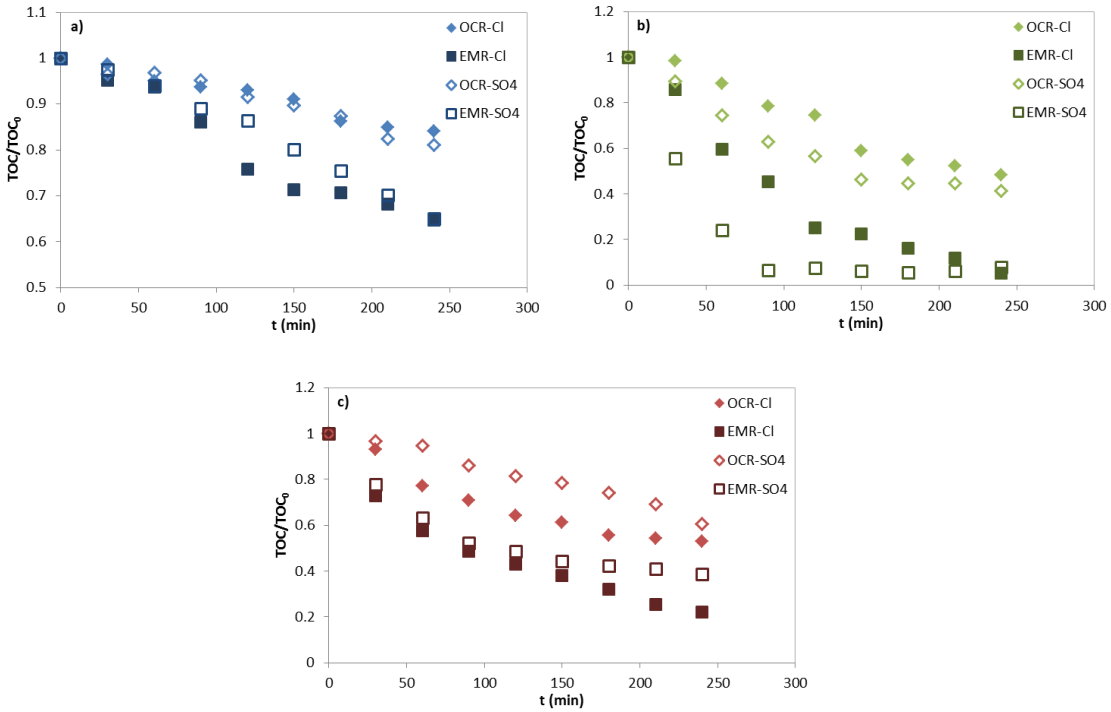

309 **Fig. 7:** TOC/TOC_0 decay profile as a function of the reactor employed (OCR and EMR) for both
310 chloride (full marks) and sulphate media (empty marks) and the different anode materials:
311 CuO (a)), BDD (b)), Sb_2O_3 (c)).
312

313 Furthermore, the analysis of some figures of merit comparing the behaviour of both reactors
314 using these two electrolytes is also performed in order to obtain a deeper knowledge about the
315 different electrodes performance to select the better working conditions. As the behaviour
316 showed by all the anodes presented the same trends, Fig. 8 depicts the evolution of the
317 electrochemical extent, mineral current efficiency and specific energy consumption only for the
318 BCE. Concerning ϕ, Fig. 8 a), the use of an EMR enhances this parameter as the TOC depletion
319 increases more than NOR degradation. Additionally, this parameter increases with time,
320 indicating that the NOR and its larger intermediates degradation occur faster than its complete
321 mineralization. The use of the chloride media slightly increases ϕ with the ceramic electrodes
322 but not for the BDD (not shown) due to its higher inactivity and oxidizing power, as
323 aforementioned. Ordering the anodes according to this parameter, BDD>BCE>CuO.

Regarding the MCE, Fig 8 b), it decreases with time independently of the reactor or electrolyte employed, which is typical behaviour of an electrolysis under mass transfer control. The use of an EMR greatly increases this parameter as it avoids the parasitic cathodic reactions, such as the destruction of the oxidant or the recombination of organic by-products. In this case, the use of chloride media highly increases this parameter as the main N-ion obtained in sulphate media, NH_4^+, (Mora-Gomez et al., 2019) changed to NO_3^-, causing the increase of the electrons involved in the NOR complete mineralization from 66 to 90. In this case, the BCE shows similar results as those obtained by BDD (not shown).

Finally, the energy consumption, Fig. 8 c), increased with time as both NOR and TOC concentration decreased since more energy was wasted in parallel reactions, and the probability of reaction among oxidants also grew. Despite of the higher current efficiency obtained with the use of the EMR, the energy consumed increased up to six times due to the overvoltage caused by the membrane presence together with the higher separation between electrodes. In this case, chloride media provided lower energy consumption as they generate more conductive ions during its oxidation in relation to the sulphate one. BCE brought the lowest energy values since was the more conductive electrode and, consequently, the cell potential was lower.

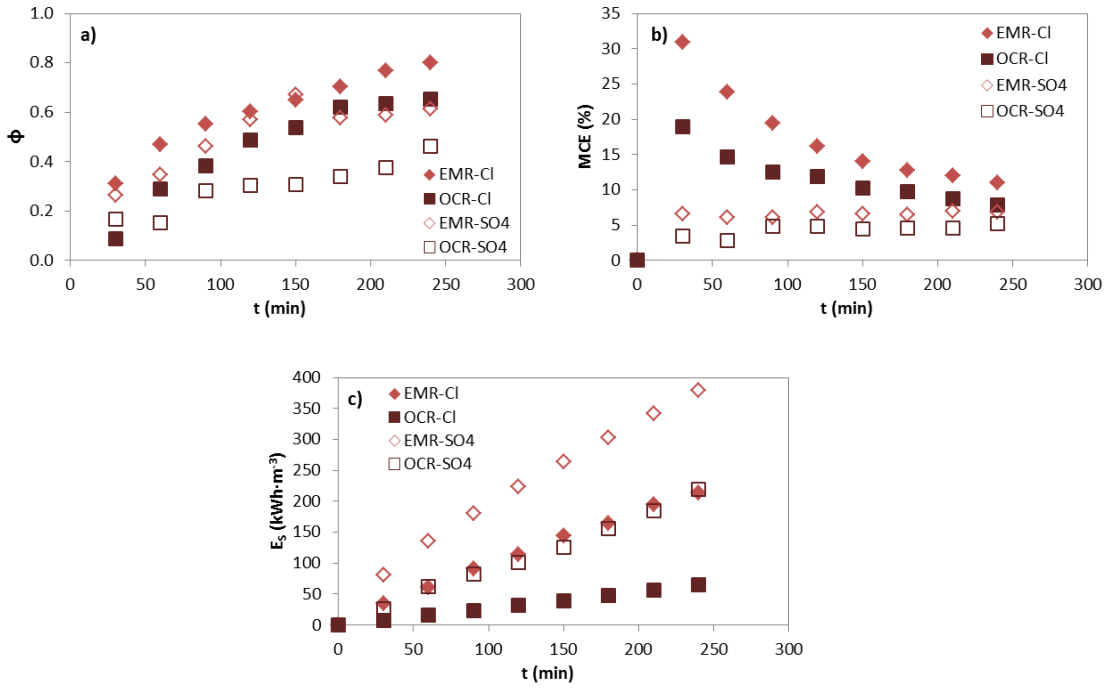

344 **Fig. 8:** Electrochemical combustion extent, a), mineralization current efficiency, b) and specific
345 energy consumption, c). obtained for the BCE electrode as a function of the reactor employed
346 (OCR and EMR) and for both chloride (full marks) and sulphate media (empty marks).

347

348 4- **Conclusions**

349

350 This work consists of the performance evaluation of three different electrode materials using
351 two different electrochemical reactors. Furthermore, the influence of two different supporting
352 electrolytes was also studied. First of all, from the electrolysis experiments carried out it was
353 clearly demonstrated that the membrane presence not only enhances NOR degradation but also
354 it improved TOC mineralization. This is thanks to the prevention of the parallel reactions that
355 can occur on the cathode. Concerning to their oxidative power, the electrodes can be ordered
356 as follows: BDD>BCE>CuO.

357 From the intermediates detected, it was observed that the NOR degradation pathway changed
358 as a function of the electrochemical reactor employed, which is corroborated by the different

359 UV-spectra obtained for both reactors. Furthermore, the main N-ion formed after NOR oxidation
360 changed from ammonia in sulphate media to nitrite/nitrate in chloride one. The higher the
361 oxidative power of the anode employed, which was enhanced by the EMR use, the higher the
362 amount of nitrate ions formed. From the electrolyte dechlorination it was concluded that both
363 ceramic electrodes presented a lower generation of oxidizing species than BDD anode.

364 Finally, the use of a BCE using an EMR appears as an interesting alternative since although the
365 membrane increased the energy consumption, it was lower than for BDD-EMR, and the MCE
366 obtained was similar to the one presented for the BDD-OCR.

367

368 **Acknowledgements**

369 The authors want to express their gratitude to the Ministerio de Economía y Competitividad
370 (Spain) and the FEDER funds, which financially support the project RTI2018-101341-B-C21.

371

372 **References**

373

374 Brillas, E., Sire, I., Oturan, M.A., Sirés, I., Oturan, M.A., 2009. Electro-Fenton Process and
375 Related Electrochemical Technologies Based on Fenton ’s Reaction Chemistry. Chem. Rev.
376 109, 6570–6631. https://doi.org/10.1021/cr900136g

377 C. Dodd, M., D. Shah, A., von Gunten, U., Huang, C.-H., 2005. Interactions of Fluoroquinolone
378 Antibacterial Agents with Aqueous Chlorine: Reaction Kinetics, Mechanisms, and
379 Transformation Pathways. Environ. Sci. & Technol. 39, 7065–7076.
380 https://doi.org/10.1021/es050054e

Carlesi Jara, C., Fino, D., Specchia, V., Saracco, G., Spinelli, P., 2007. Electrochemical removal of antibiotics from wastewaters. Appl. Catal. B Environ. 70, 479–487. https://doi.org/10.1016/j.apcatb.2005.11.035

Coledam, D.A.C., Aquino, J.M., Silva, B.F., Silva, A.J., Rocha-Filho, R.C., 2016. Electrochemical mineralization of norfloxacin using distinct boron-doped diamond anodes in a filter-press reactor, with investigations of toxicity and oxidation by-products. Electrochim. Acta 213, 856–864. https://doi.org/10.1016/j.electacta.2016.08.003

Coledam, D.A.C., Sánchez-Montes, I., Silva, B.F., Aquino, J.M., 2018. On the performance of HOCl/Fe2+, HOCl/Fe2+/UVA, and HOCl/UVC processes using in situ electrogenerated active chlorine to mineralize the herbicide picloram. Appl. Catal. B Environ. 227, 170–177. https://doi.org/10.1016/j.apcatb.2017.12.072

Comninellis, C. and G.C., 2010. Electrochemistry for the environment. Springer New York, New York. https://doi.org/10.1007/978-0-387-68318-8

da Silva, S.W., Navarro, E.M.O., Rodrigues, M.A.S., Bernardes, A.M., Pérez-Herranz, V., 2018. The role of the anode material and water matrix in the electrochemical oxidation of norfloxacin. Chemosphere 210, 615–623. https://doi.org/10.1016/j.chemosphere.2018.07.057

Ghernaout, D., Naceur, M.W., Aouabed, A., 2011. On the dependence of chlorine by-products generated species formation of the electrode material and applied charge during electrochemical water treatment. Desalination 270, 9–22. https://doi.org/10.1016/j.desal.2011.01.010

Guinea, E., Garrido, J.A., Rodríguez, R.M., Cabot, P.-L., Arias, C., Centellas, F., Brillas, E., 2010. Degradation of the fluoroquinolone enrofloxacin by electrochemical advanced oxidation processes based on hydrogen peroxide electrogeneration. Electrochim. Acta 55, 2101–

2115. https://doi.org/10.1016/j.electacta.2009.11.040

Guo, H., Gao, N., Yang, Y., Zhang, Y., 2016. Kinetics and Transformation Pathways on Oxidation of Fluoroquinolones with Thermally Activated Persulfate. Chem. Eng. J. https://doi.org/10.1016/j.cej.2016.01.009

Guzmán-Duque, F.L., Palma-Goyes, R.E., González, I., Peñuela, G., Torres-Palma, R.A., 2014. Relationship between anode material, supporting electrolyte and current density during electrochemical degradation of organic compounds in water. J. Hazard. Mater. 278, 221–226. https://doi.org/10.1016/j.jhazmat.2014.05.076

Huang, K.-J., Liu, X., Xie, W.-Z., Yuan, H.-X., 2008. Electrochemical behavior and voltammetric determination of norfloxacin at glassy carbon electrode modified with multi walled carbon nanotubes/Nafion. Colloids Surf. B. Biointerfaces 64, 269–74. https://doi.org/10.1016/j.colsurfb.2008.02.003

Jojoa-Sierra, S.D., Silva-Agredo, J., Herrera-Calderon, E., Torres-Palma, R.A., 2017. Elimination of the antibiotic norfloxacin in municipal wastewater, urine and seawater by electrochemical oxidation on IrO 2 anodes. Sci. Total Environ. 575, 1228–1238. https://doi.org/10.1016/j.scitotenv.2016.09.201

Liu, C., Nanaboina, V., Korshin, G. V., Jiang, W., 2012. Spectroscopic study of degradation products of ciprofloxacin, norfloxacin and lomefloxacin formed in ozonated wastewater. Water Res. 46, 5235–5246. https://doi.org/10.1016/J.WATRES.2012.07.005

Ma, X., Cheng, Y., Ge, Y., Wu, H., Li, Q., Gao, N., Deng, J., 2018. Ultrasound-enhanced nanosized zero-valent copper activation of hydrogen peroxide for the degradation of norfloxacin. Ultrason. Sonochem. 40, 763–772. https://doi.org/10.1016/j.ultsonch.2017.08.025

Madsen, H.T., Søgaard, E.G., Muff, J., 2015. Study of degradation intermediates formed during electrochemical oxidation of pesticide residue 2,6-dichlorobenzamide (BAM) in chloride medium at boron doped diamond (BDD) and platinum anodes. Chemosphere 120, 756–763. https://doi.org/10.1016/J.CHEMOSPHERE.2014.10.058

Martínez-Huitle, C.A., Panizza, M., 2018. Electrochemical oxidation of organic pollutants for wastewater treatment. Curr. Opin. Electrochem. 11, 62–71. https://doi.org/10.1016/J.COELEC.2018.07.010

Mora-Gómez, J., García-Gabaldón, M., Ortega, E., Sánchez-Rivera, M.J., Mestre, S., Pérez-Herranz, V., 2018. Evaluation of new ceramic electrodes based on Sb-doped SnO2for the removal of emerging compounds present in wastewater. Ceram. Int. 44, 2216–2222. https://doi.org/10.1016/j.ceramint.2017.10.178

Mora-Gomez, J., Ortega, E., Mestre, S., Pérez-Herranz, V., García-Gabaldón, M., 2019. Electrochemical degradation of norfloxacin using BDD and new Sb-doped SnO2 ceramic anodes in an electrochemical reactor in the presence and absence of a cation-exchange membrane. Sep. Purif. Technol. 208, 68–75. https://doi.org/10.1016/j.seppur.2018.05.017

Mora-Gómez, J., García-Gabaldón, M., Carrillo-Abad, J., Montañés, M.T., Mestre, S., Pérez-Herranz, V., 2020. Influence of the reactor configuration and the supporting electrolyte concentration on the electrochemical oxidation of Atenolol using BDD and SnO2 ceramic electrodes. Sep. Purif. Technol. 241, 116684. https://doi.org/10.1016/J.SEPPUR.2020.116684

Murugananthan, M., Latha, S.S., Bhaskar Raju, G., Yoshihara, S., 2011. Role of electrolyte on anodic mineralization of atenolol at boron doped diamond and Pt electrodes. Sep. Purif. Technol. 79, 56–62.

https://doi.org/10.1016/J.SEPPUR.2011.03.011

Özcan, A., Atılır Özcan, A., Demirci, Y., 2016. Evaluation of mineralization kinetics and pathway of norfloxacin removal from water by electro-Fenton treatment. Chem. Eng. J. 304, 518–526. https://doi.org/10.1016/j.cej.2016.06.105

Sánchez-Montes, I., Fuzer Neto, J.R., Silva, B.F., Silva, A.J., Aquino, J.M., Rocha-Filho, R.C., 2018. Evolution of the antibacterial activity and oxidation intermediates during the electrochemical degradation of norfloxacin in a flow cell with a PTFE-doped β-PbO2anode: Critical comparison to a BDD anode. Electrochim. Acta 284, 260–270. https://doi.org/10.1016/j.electacta.2018.07.122

Santos, I.D., Gabriel, S.B., Afonso, J.C., Dutra, A.J.B., 2011. Preparation and characterization of Ti/SnO2-Sb electrode by Pechini's method for phenol oxidation. Mater. Res. 14, 408–416. https://doi.org/10.1590/S1516-14392011005000054

Sopaj, F., Rodrigo, M.A., Oturan, N., Podvorica, F.I., Pinson, J., Oturan, M.A., 2015. Influence of the anode materials on the electrochemical oxidation efficiency. Application to oxidative degradation of the pharmaceutical amoxicillin. Chem. Eng. J. 262, 286–294. https://doi.org/10.1016/j.cej.2014.09.100

Tong, S.-P., Ma, C.-A., Feng, H., 2008. A novel PbO2 electrode preparation and its application in organic degradation. Electrochim. Acta 53, 3002–3006. https://doi.org/10.1016/J.ELECTACTA.2007.11.011

Urtiaga, A., Soriano, A., Carrillo-Abad, J., 2018. BDD anodic treatment of 6:2 fluorotelomer sulfonate (6:2 FTSA). Evaluation of operating variables and by-product formation. Chemosphere 201. https://doi.org/10.1016/j.chemosphere.2018.03.027

Wang, Y., Shen, C., Zhang, M., Zhang, B.T., Yu, Y.G., 2016. The electrochemical degradation of

ciprofloxacin using a SnO2-Sb/Ti anode: Influencing factors, reaction pathways and energy demand. Chem. Eng. J. 296, 79–89. https://doi.org/10.1016/j.cej.2016.03.093

Wu, M., Zhao, G., Li, M., Liu, L., Li, D., 2009. Applicability of boron-doped diamond electrode to the degradation of chloride-mediated and chloride-free wastewaters. J. Hazard. Mater. 163, 26–31. https://doi.org/10.1016/J.JHAZMAT.2008.06.050

Zhao, G., Zhang, Yonggang, lei, Y., Lv, B., Gao, J., Zhang, Yanan, Li, D., 2010. Fabrication and Electrochemical Treatment Application of A Novel Lead Dioxide Anode with Superhydrophobic Surfaces, High Oxygen Evolution Potential, and Oxidation Capability. Environ. Sci. & Technol. 44, 1754–1759. https://doi.org/10.1021/es902336d